

# Molecular Dynamics Simulations Predict a Favorable and Unique Mode of Interaction between Lithium ( $\text{Li}^+$ ) Ions and Hydrophobic Molecules in Aqueous Solution

Andrew S. Thomas and Adrian H. Elcock\*

Department of Biochemistry, University of Iowa, Iowa City, Iowa 52242, United States

**S** Supporting Information

**ABSTRACT:** We report the results of molecular dynamics simulations of the interaction thermodynamics of group I cations with hydrophobic molecules in water using a variety of nonpolarizable force fields. Surprisingly, we find that the  $\text{Li}^+$  ion is predicted to form thermodynamically favorable interactions with methane and neopentane using a new mode of recognition that is intermediate between a direct contact and a solvent-separated complex. Further simulations show that this favorable interaction is only predicted by ion parameter sets that correctly reproduce  $\text{Li}^+$ 's experimental hydration number.

## INTRODUCTION

While the behavior of ions in aqueous solution has long been subjected to study through both theory and experiment,<sup>1</sup> only recently have force field parameters for ions reached a level of maturity at which molecular simulation methods can reproduce simultaneously both the thermodynamic and structural features of the ion–water interaction.<sup>2</sup> The development of accurate parameter sets for the group I cations, in particular, opens the way to a detailed study of their interactions with other biomolecular solutes in aqueous solution. As one step in this direction, we have used a series of long molecular dynamics (MD) simulations to undertake a comparative study of the interaction thermodynamics of three group I cations,  $\text{Li}^+$ ,  $\text{Na}^+$ , and  $\text{K}^+$ , with hydrophobic molecules in water.

The few previous computational studies examining interactions between ions and hydrophobic molecules have suggested that their nature can depend significantly on the size of the ion. Using a simplified 2D water model, Hribar et al.<sup>3</sup> showed that in an aqueous solution containing a small, charge-dense cation (reminiscent of  $\text{Li}^+$ ) an inserted hydrophobic solute preferred to adopt a solvent-separated configuration relative to the ion; in contrast, when a larger, charge-diffuse cation (similar to  $\text{Cs}^+$ ) was present in the solution, the hydrophobic solute was observed to penetrate the hydration shell of the ion and “bind” to the ion's surface. Following that work, others have used more conventional molecular dynamics (MD) simulations to model interactions between ions and hydrophobic groups. Shinto et al.<sup>4</sup> explored how the ions  $\text{Na}^+$ ,  $\text{Cl}^-$ , and tetramethylammonium,  $(\text{CH}_3)_4\text{N}^+$ , interact with a united-atom model of methane. In the case of the comparatively small, charge-dense ion,  $\text{Na}^+$ , a thermodynamically favorable solvent-separated interaction was observed, but closer interaction, in the form of a direct contact between the ion and the methane, was apparently prevented due (presumably) to the energetically unfavorable desolvation that would be incurred by the ion. In the case of the much larger, charge-diffuse tetramethylammonium ion, however, direct binding to the methane was observed, in a manner qualitatively

similar to the conventional association of two hydrophobic molecules. Similar observations were reported by Lund et al.<sup>5</sup> for interactions of monovalent anions ( $\text{F}^-$  and  $\text{I}^-$ ) with a nanometer-sized hydrophobic solute; again, the charge-dense  $\text{F}^-$  ion was effectively excluded from the nonpolar surface, while the charge-diffuse  $\text{I}^-$  ion bound quite readily. Taken together therefore, all of these previous works suggest a simple, general rule for ion–hydrophobe interactions: large, charge-diffuse ions have the potential to bind directly to hydrophobic groups, but small, charge-dense ions do not (although they may adopt favorable solvent-separated configurations).<sup>3–5</sup>

The molecular simulations reported here provide evidence that this line of thinking may not always be appropriate: the simulations predict a surprising, thermodynamically favorable interaction between the small, charge-dense  $\text{Li}^+$  ion and hydrophobic molecules in aqueous solution. We further show that this favorable interaction is a robust prediction of all tested force fields that correctly reproduce the hydration number of the  $\text{Li}^+$  ion.

## METHODS

Free energies of interaction between ions and hydrophobic molecules were obtained from explicit solvent MD simulations performed with the GROMACS 4.0 software.<sup>6</sup> In all simulations, a single hydrophobic solute (methane or neopentane) and a single ion were placed in a  $25 \times 25 \times 25$  Å simulation box containing approximately 500 explicitly modeled water molecules such that the overall density was 1 g/cm<sup>3</sup>. For each type of ion, independent simulations were performed with all three of the ion parameter sets recently derived by Joung and Cheatham,<sup>2</sup> these three sets have been developed for use, respectively, with the SPC/E,<sup>7</sup> TIP3P,<sup>8</sup> and TIP4P-Ew<sup>9</sup> water models. In the case of the  $\text{Li}^+$  ion, simulations were also performed with Åqvist's ion parameters<sup>10</sup> in combination with SPC/E, SPC,<sup>11</sup> and TIP3P

**Received:** September 14, 2010

**Published:** March 03, 2011

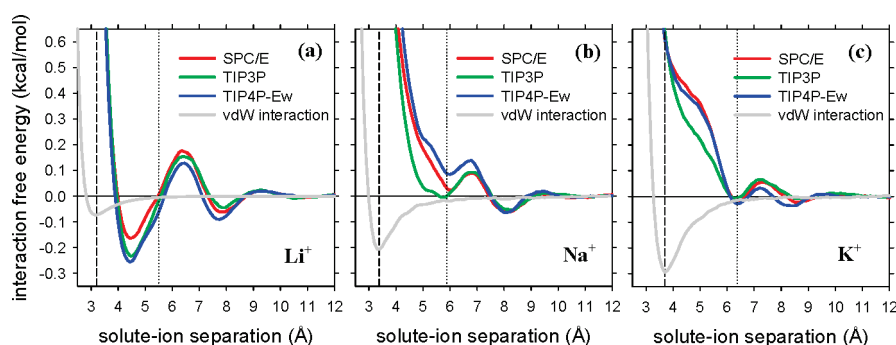


**Figure 1.** Computed interaction free energies for the association of methane with (a)  $\text{Li}^+$ , (b)  $\text{Na}^+$ , and (c)  $\text{K}^+$  as a function of the ion–methane distance. The red, green, and blue lines show results obtained with Joung and Cheatham’s ion parameters specifically derived for use with the water models identified in the inset. The solid gray line in each figure is the direct interaction between the ion and the hydrophobic solute calculated in vacuum. The positions of the van der Waals contact minimum (CM) and the solvent-separated minimum (SSM) are indicated by dashed and dotted vertical lines, respectively. The expected position of a SSM for  $\text{Li}^+$  is shown as 2.34 Å further than the CM position; this is based on a linear fit between the positions of the SSM and the first peak in the cation–water radial distribution function for the three group I cations. Error bars for each data set are not shown for purposes of clarity; however, they amount to less than 0.05 kcal/mol.

water, and with Jensen and Jorgensen’s ion parameters<sup>12</sup> in TIP4P water.<sup>8</sup> The hydrophobic solutes methane and neopentane were both described using parameters from the OPLS all-atom force field;<sup>13</sup> additional simulations of the  $\text{Li}^+$ –methane interaction were also performed with methane described by the OPLS united-atom force field.<sup>14</sup> To be consistent with the parametrization of the respective ions, the Lorentz–Berthelot<sup>2</sup> or geometric<sup>10,12</sup> mixing rules were used for all van der Waals interactions that involved ions; to be consistent with the OPLS parametrization scheme,<sup>13</sup> geometric mixing rules were used to describe van der Waals interactions between the hydrophobic solutes and water.

All MD simulations used a standard protocol. Short-range non-bonded interactions were directly calculated up to a 10 Å cutoff; long-range electrostatic interactions beyond this cutoff were calculated using the particle mesh Ewald (PME) method.<sup>15</sup> The temperature was maintained at 298 K using the Nosé–Hoover thermostat,<sup>16</sup> and pressure was maintained at 1 atm using the Parrinello–Rahman barostat.<sup>17</sup> Covalent bonds in the methane were constrained using the LINCS algorithm,<sup>18</sup> allowing for a 2 fs time step to be used. Simulations were first heated up to 298 K over the course of 1 ns, then equilibrated for a further 10 ns, before “production” simulations of 500 ns were conducted. As we have shown previously,<sup>19</sup> these long simulation times allow for converged estimates of the association thermodynamics to be calculated directly from completely unbiased MD simulations. In the present study, the free energy of interaction,  $\Delta G$ , as a function of the ion–hydrophobe distance was determined from the calculated radial distribution function,  $g(r)$ , of the central carbon-to-ion distance using  $\Delta G = -RT \ln g(r)$ . Radial distribution functions were calculated using the *g\_rdf* utility of GROMACS.<sup>6</sup>

Since the results obtained from the above simulations turned out to be so surprising in the case of  $\text{Li}^+$  (see the Results), a large number of additional control simulations of the  $\text{Li}^+$ –methane system were performed to establish the robustness of the predicted behavior. To rule out an influence from the choice of mixing rules used to describe the ion–hydrophobe van der Waals interactions, additional simulations were performed using alternative mixing rules (see the Supporting Information for details). To explore the role of the van der Waals parameters assigned to the methane, additional simulations were performed using AMBER99 van der Waals parameters<sup>20</sup> (see Figure S1, Supporting Information). Finally, at the behest of a reviewer, additional simulations were performed with a larger, 35 Å simulation box

(Figure S2, Supporting Information). As shown in the Supporting Information, all of these control simulations produced results qualitatively identical with the results reported herein.

In order to explore the sensitivity of the observed behavior of  $\text{Li}^+$  to the presence of additional salt, MD simulations of the  $\text{Li}^+$ –methane interaction were also performed in a 1 M  $\text{LiCl}$  solution; these simulations involved the addition of eight  $\text{Li}^+$  and nine  $\text{Cl}^-$  ions to the system but were run in an otherwise identical manner to those conducted in pure water. Finally, to explore whether results similar to those obtained with the  $\text{Li}^+$ –methane system might also be found in some other systems MD simulations were used to study the interaction thermodynamics of methane with the  $\text{NH}_4^+$  cation,<sup>13</sup> and with the  $\text{F}^-$  anion;<sup>2</sup> independent simulations of the latter interactions were performed using all three of the Joung and Cheatham parameter sets.

## RESULTS AND DISCUSSION

The interaction free energies computed for methane’s interaction with  $\text{Li}^+$ ,  $\text{Na}^+$ , and  $\text{K}^+$  in water are plotted as a function of the ion–hydrophobe separation distance in Figure 1a, b, and c, respectively. The colored lines in each panel show the results computed with the three water model-dependent ion parameter sets developed by Joung and Cheatham;<sup>2</sup> clearly, all three parameter sets give very similar results (corresponding results obtained with other parameter sets are considered later in this manuscript). The most surprising and interesting results of the simulations reported here are to be found in the plots of the  $\text{Li}^+$ –methane interaction free energy versus the distance (Figure 1a). Two aspects of these plots are particularly notable. First, the  $\text{Li}^+$ –methane interaction is predicted to be thermodynamically favorable at distances between 4.0 and 5.5 Å, with a strength approximately one-third that of the more conventional hydrophobic interaction between two methane molecules.<sup>21</sup> This observation of a thermodynamically favorable interaction between  $\text{Li}^+$  and methane is a major surprise since, as noted in the Introduction, the conventional view of ion–hydrophobe interactions is that they should be thermodynamically unfavorable, owing to the cost of disrupting the ion’s hydration shell.<sup>3</sup> Certainly, this conventional thinking is borne out for methane’s interaction with both  $\text{Na}^+$  (Figure 1b) and  $\text{K}^+$  (Figure 1c): neither ion shows a tendency to form a short-range favorable

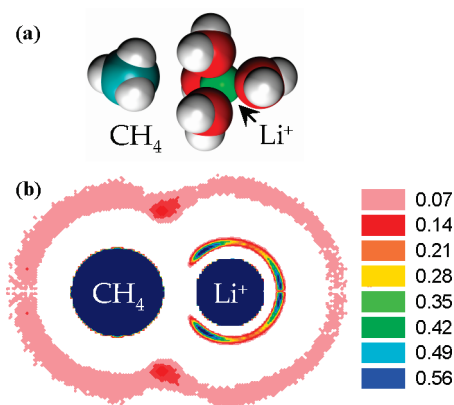


**Figure 2.** (a) MD snapshot of the  $\text{Li}^+$ –methane complex at its free energy minimum configuration. (b) 2-D projection of water density around the free energy minimum configuration (molecules/ $\text{\AA}^3$ ). This plot was computed using all snapshots in which the  $\text{Li}^+$ –methane separation was 4.5–4.6  $\text{\AA}$  in the MD simulation that used the Joung and Cheatham SPC/E parameters. Essentially identical results were obtained using Joung and Cheatham’s TIP3P and TIP4P-Ew parameters.

interaction with the hydrophobic molecule. But since  $\text{Li}^+$  is the most charge-dense of the group I cations,<sup>1</sup> it would be expected to be even more adversely affected by the approach of a nonpolar molecule than either  $\text{Na}^+$  or  $\text{K}^+$ . The simulation results shown in Figure 1a, however, clearly challenge this notion.

The second notable aspect of the results obtained for the  $\text{Li}^+$ –methane interaction (Figure 1a) is that the distance at which the interaction is most favorable ( $\sim 4.5$   $\text{\AA}$ ) corresponds to neither of the two usual modes of molecular interaction: it is too long to be a direct van der Waals contact interaction (indicated by the solid gray curve in Figure 1a) and too short to be a solvent-separated interaction of the type sometimes observed with other ions (the expected position of this minimum is indicated by the dotted gray vertical line). Instead, an examination of “snapshots” taken from the simulations shows that at this separation distance the  $\text{Li}^+$  ion retains a tetrahedrally coordinated hydration shell<sup>1</sup> by approaching the hydrophobic molecule along a line trisecting three of the  $\text{Li}^+$ – $\text{H}_2\text{O}$  “bonds” (Figure 2a). As a result, the complex encloses a  $\sim 1.5$ - $\text{\AA}$ -long region of the vacuum separating the ion from its hydrophobic binding partner.

A more quantitative illustration of the water distribution around the  $\text{Li}^+$ –methane complex can be obtained from the two-dimensional projection of the water oxygen density shown in Figure 2b. This plot clearly hints at the retention of the highly structured first hydration shell around the  $\text{Li}^+$  ion and also shows, interestingly, that water density is increased significantly (by a factor of  $\sim 2$ ) in the region where the methane’s first hydration shell intersects with the diffuse second hydration shell of the  $\text{Li}^+$  ion. Aside from this latter effect, however, the  $\text{Li}^+$  ion does not appear to induce significant additional structuring of the water surrounding the hydrophobic molecule. The retention of the tetrahedral hydration waters, even in complex with methane, suggests therefore that  $\text{Li}^+$  acts as a “permanently” hydrated ion  $[\text{Li}-(\text{H}_2\text{O})_4]^+$  in solution, similar to some small divalent and trivalent ions.<sup>22</sup>

Although it is often difficult to distinguish cause from effect when analyzing simulated behavior, we have attempted to identify the factors that drive the formation of the favorable  $\text{Li}^+$ –methane contact by decomposing the interaction thermodynamics into individual energetic components. To this end, we have taken 5 million structural snapshots from each simulation and extracted the

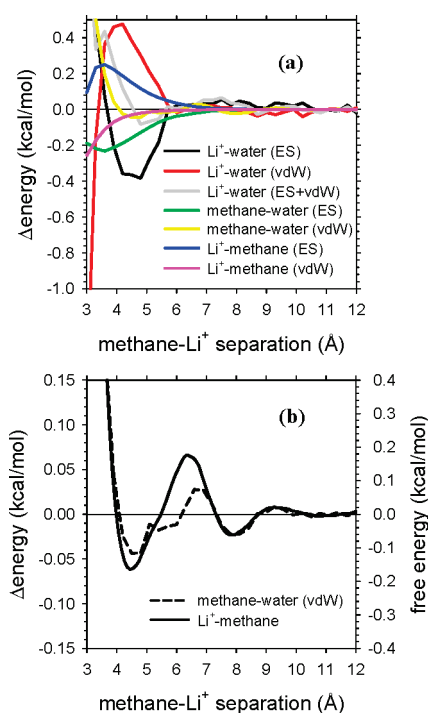


**Figure 3.** (a) Energetic contributions to the  $\text{Li}^+$ –methane interaction plotted as a function of the  $\text{Li}^+$ –methane distance. Lines shown correspond to data from simulations that used the Joung and Cheatham SPC/E parameter set. (b) The change in the methane–water van der Waals interaction energy as a function of the  $\text{Li}^+$ –methane distance is plotted as a dashed line against the left-hand y axis (these data are replotted from part a); for comparison, the interaction free energy as a function of the  $\text{Li}^+$ –methane distance is plotted as a solid line against the right-hand y axis (these data are replotted from Figure 1a).

electrostatic and van der Waals components of each of the following interactions: (a)  $\text{Li}^+$ –water, (b)  $\text{Li}^+$ –methane, and (c) methane–water; the results of this analysis for the SPC/E set of Joung and Cheatham parameters are shown in Figure 3 (corresponding results for the other Joung and Cheatham parameter sets are shown in Figure S3, Supporting Information). Interestingly, the  $\text{Li}^+$ –water electrostatic interaction energy becomes significantly more favorable as the  $\text{Li}^+$  and methane approach one another and reaches its minimum value (stabilized by  $-0.4$  kcal/mol) when the  $\text{Li}^+$ –methane distance reaches its free energy minimum distance (4.5  $\text{\AA}$ ). This favorable change in energy is opposed by a corresponding unfavorable change in the  $\text{Li}^+$ –water van der Waals interaction (compare red and black lines in Figure 3a), but the net effect (i.e., the sum of the electrostatic and van der Waals terms) is a slightly favorable contribution to the interaction, albeit one that reaches a minimum value at a somewhat farther distance ( $\sim 5$   $\text{\AA}$ ) than the free energy minimum distance. Similar effects, but differing markedly in magnitude, are seen with the other Joung and Cheatham parameter sets (see Figures S3a and b, Supporting Information). The methane–water electrostatic interaction (green line) also becomes more energetically favorable as the  $\text{Li}^+$  and methane approach one another and is most favorable when the two are in direct contact with one another; this component, however, appears to be effectively canceled by a corresponding unfavorable change in the  $\text{Li}^+$ –methane electrostatic interaction (blue line). As expected, the  $\text{Li}^+$ –methane van der Waals interaction (pink line) becomes increasingly favorable as the two molecules approach, but its contribution is very small at a separation distance of 4.5  $\text{\AA}$  ( $-0.03$  kcal/mol) and is not likely,

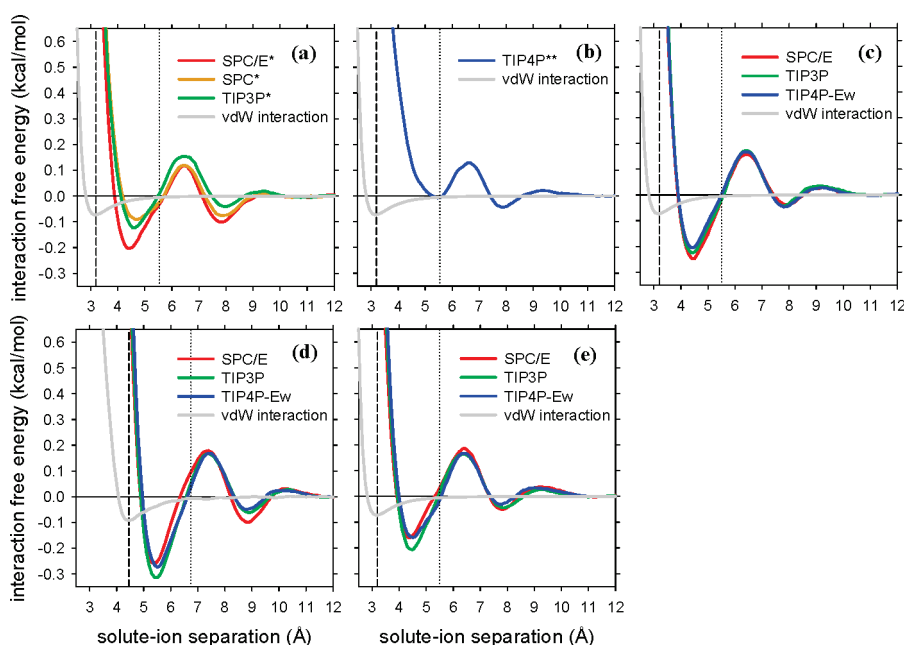


**Figure 4.** Computed interaction free energies for the association of  $\text{Li}^+$  with (a) methane using Åqvist's (denoted \*) ion parameters, (b) methane using Jensen and Jorgensen's (denoted \*\*) ion parameters, (c) united-atom methane using Joung and Cheatham's ion parameters, (d) neopentane using Joung and Cheatham's ion parameters, and (e) methane in 1 M LiCl solution using Joung and Cheatham's ion parameters.

therefore, to be a significant determinant of the favorable  $\text{Li}^+$ –methane interaction. The final energetic contribution to consider is the methane–water van der Waals interaction (yellow line in Figure 3a). Intriguingly, the shape of this curve follows the free energy curve very nicely with all three of the Joung and Cheatham parameter sets (see Figure 3b and Figure S3c and d, Supporting Information), which suggests that this interaction is a potential determinant of the observed interaction thermodynamics. A more complete analysis of the underlying thermodynamics would, of course, require an analysis of entropic contributions (see e.g. refs 23 and 24), but that is beyond the scope of the present work.

Since the prediction of a thermodynamically favorable  $\text{Li}^+$ –methane interaction is a major surprise and is likely to be controversial, we have been careful to explore whether its prediction is robust to changes in the simulation parameters. Figure 4a shows the results computed using parameters for  $\text{Li}^+$  derived by Åqvist; since his ion parameter set has been used in conjunction with a number of three-site water models in the literature, we performed independent simulations with each of the TIP3P, SPC, and SPC/E water models. With all three models, we again obtain a thermodynamically favorable interaction at a separation distance of  $\sim 4.5$  Å (Figure 4a). Interestingly, however, the interaction free energy is computed to be significantly more favorable with the SPC/E model than with either of the other two water models; a likely explanation for this result is outlined below.

Figure 4b shows the results computed using  $\text{Li}^+$  parameters derived by Jensen and Jorgensen.<sup>12</sup> In this case, it is clear that a thermodynamically favorable  $\text{Li}^+$ –methane interaction is not predicted. At first sight this result appears to call into question the significance of the results reported earlier. Below, however, we present evidence that this particular parameter set may be compromised by having been derived to fit experimental data that have since been subject to revision.

Figure 4c shows the results computed using Joung and Cheatham's  $\text{Li}^+$  parameters in combination with an OPLS

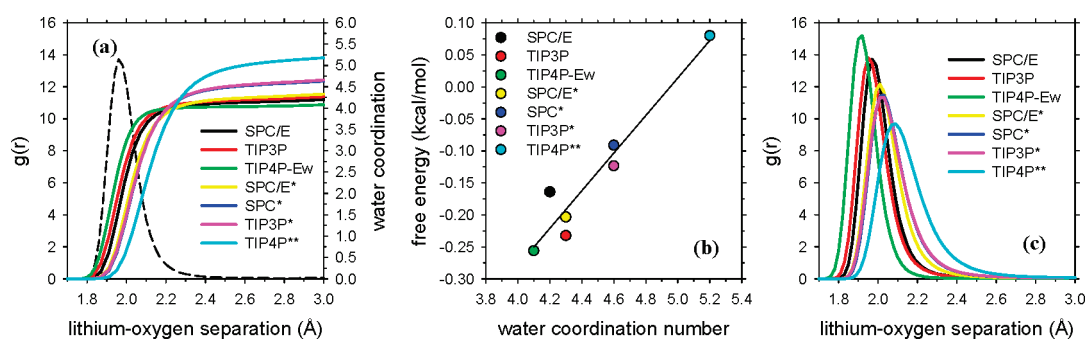
united-atom description for the methane.<sup>14</sup> In this case, results essentially identical to those obtained with the all-atom methane model are obtained, indicating that the observed interaction is not dependent on the details of the methane's modeling. The results of additional simulations, which explored (a) changing the mixing rules used to describe van der Waals interactions and (b) increasing the simulation box size, are shown in Figures S1 and S2, Supporting Information, respectively; neither change resulted in any significant change to the computed thermodynamics of the  $\text{Li}^+$ –methane interaction.

Figure 4d shows the results computed using Joung and Cheatham's ion parameters in simulations of the interaction of  $\text{Li}^+$  with the larger hydrophobic molecule neopentane. From this, it is clear that the prediction of a thermodynamically favorable interaction between the  $\text{Li}^+$  ion and a hydrophobic molecule is not restricted to methane; the  $\text{Li}^+$ –neopentane interaction free energy is, in fact, predicted to be somewhat more favorable ( $-0.25$  to  $-0.30$  kcal/mol).

Finally, Figure 4e shows the results computed using Joung and Cheatham's ion parameters in simulations of the  $\text{Li}^+$ –methane interaction in a 1 M LiCl solution. Again, a favorable  $\text{Li}^+$ –methane interaction is retained: even competition from halide ions, therefore, appears unable to completely suppress the ion–hydrophobe interaction.

Focusing again on those panels of Figures 1 and 4 that plot the computed free energies of the  $\text{Li}^+$ –methane interaction in pure water, we can make the following statements: (a) The most favorable  $\text{Li}^+$ –methane interactions are predicted by the three Joung and Cheatham parameter sets and by Åqvist's parameters when used with the SPC/E water model. (b) Somewhat weaker but still favorable  $\text{Li}^+$ –methane interactions are predicted by Åqvist's parameters when used with the SPC and TIP3P water models. (c) A favorable  $\text{Li}^+$ –methane interaction is not predicted by the Jensen and Jorgensen parameters. Since these are significant discrepancies, it is important both to try to identify





**Figure 5.** Effects of ion and water model parameters on the Li<sup>+</sup> hydration structure. (a) Li<sup>+</sup>–water coordination numbers (plotted against the right-hand y axis) and the Li<sup>+</sup>–water oxygen radial distribution function in SPC/E (left-hand y axis, dashed line), both plotted as a function of the Li<sup>+</sup>–water oxygen distance. (b) Correlation between the free energy at the Li<sup>+</sup>–methane free energy minimum (at a separation of 4.55 Å) and the Li<sup>+</sup>–water coordination number computed with the same parameter set. (c) Li<sup>+</sup>–water oxygen radial distribution functions plotted as a function of the Li<sup>+</sup>–water oxygen distance. The water model-dependent ion parameters of Joung and Cheatham, Åqvist (denoted \*), and Jensen and Jorgensen (denoted \*\*) were used.

their origins and to determine which of the predicted results is likely to be the most realistic.

In the absence of direct experimental data on the thermodynamics of the Li<sup>+</sup>–methane interaction, we must attempt to assess the quality of the various parameter sets by examining their abilities to reproduce alternative sources of experimental data. One obvious measure to consider is the hydration free energy of the Li<sup>+</sup> ion since this is likely to be a major determinant of its observed interaction thermodynamics with methane in aqueous solution. But both the Joung and Cheatham, and Jensen and Jorgensen parameter sets have been explicitly parametrized to reproduce Marcus' estimate of Li<sup>+</sup>'s hydration free energy of −113 kcal/mol,<sup>25</sup> effectively ruling this out as a possible cause of the differences observed between the two parameter sets.

A second measure that can be used to assess the quality of the various parameter sets is the water coordination number of the isolated solutes. All of the various simulation models used here predict the number of waters in the very diffuse hydration shell around methane to average ∼19–21 (Figure S4, Supporting Information). Encouragingly, these estimates are consistent both with previous computational studies<sup>26</sup> and, more importantly, with a recent experimental estimate of 20.<sup>27</sup>

But the various simulation models differ significantly in the water coordination numbers that they predict for the isolated Li<sup>+</sup> ion (see Figure 5a). The mean coordination numbers that we obtain from our simulations are, for the Joung and Cheatham Li<sup>+</sup> parameters: 4.2, 4.3, and 4.1 using the SPC/E, TIP3P, and TIP4P-Ew models, respectively; for the Åqvist Li<sup>+</sup> parameters: 4.3, 4.6, and 4.6 using the SPC/E, SPC, and TIP3P models, respectively; and for the Jensen and Jorgensen Li<sup>+</sup> parameters (in TIP4P): 5.2. All of these numbers agree well with those reported in previously published simulation studies that used the same force fields.<sup>12,28</sup> More interestingly, however, there is a clear correlation between the computed hydration numbers of the isolated Li<sup>+</sup> ion and the predicted free energy of the Li<sup>+</sup>–methane interaction obtained with the same parameter set (see Figure 5b): those parameter sets that produce lower hydration numbers predict significantly more favorable interaction free energies for the Li<sup>+</sup>–methane complex.

This trend becomes significant when we note that recent experimental studies indicate that the water coordination number of the Li<sup>+</sup> ion is 4,<sup>1,29</sup> and that similar numbers have been obtained from polarizable MD studies,<sup>30</sup> from full quantum mechanical calculations of ion–water clusters,<sup>31</sup> and from QM-MM calculations of ions in aqueous solution.<sup>32</sup> On the basis of these previous studies, therefore,

it appears that the best structural description of Li<sup>+</sup>'s hydration is provided by the three Li<sup>+</sup> parameter sets derived by Joung and Cheatham and by Åqvist's parameters when used with the SPC/E water model. All things being equal, therefore, we anticipate that the Li<sup>+</sup>–methane interaction thermodynamics predicted by the Joung and Cheatham parameter sets should be the most realistic, and that the possibility of the predicted favorable Li<sup>+</sup>–methane interaction being real is therefore significant.

The results obtained with Jensen and Jorgensen's Li<sup>+</sup> parameters suggest that the presence of an additional water molecule in the ion's hydration shell is sufficient to prevent the formation of a thermodynamically favorable Li<sup>+</sup>–methane complex. This is consistent with the clearly tetrahedral arrangement of water molecules around the Li<sup>+</sup> ion in the MD snapshots of the Li<sup>+</sup>–methane complex (Figure 2). But what is the origin of the apparently excessive hydration number obtained with the Jensen and Jorgensen parameters? It appears to be the position of the first peak in the Li<sup>+</sup>–water oxygen RDF, which was explicitly used—together with the ion's experimental hydration free energy—as a target of the parametrization process.<sup>12</sup> At the time that Jensen and Jorgensen's work was conducted, the generally accepted position of this peak—which was a weighted average of disparate experimental measurements—was at a distance of 2.08 Å for Li<sup>+</sup> in a dilute solution,<sup>33</sup> but this value has since been revised downward by 0.12 Å to ∼1.94–1.98 Å on the basis of more recent experimental measurements.<sup>1</sup> Accordingly, a comparison of the Li<sup>+</sup>–water oxygen RDFs computed with the various parameter sets used here shows that the Jensen and Jorgensen parameters produce a peak that is clearly shifted to a further distance than those obtained with other parameter sets (Figure 5c). Interestingly, the next furthest shifted peaks are those resulting from the use of Åqvist's parameters with the SPC and TIP3P models; these parameters, it will be recalled, predicted a noticeably weaker free energy for the Li<sup>+</sup>–methane interaction than was obtained with the SPC/E model (Figure 4a). There appears, therefore, to be a clear relationship between (a) the position of the first peak in the Li<sup>+</sup>–water oxygen RDF, (b) the (integrated) water coordination number, and (c) the computed thermodynamics of the Li<sup>+</sup>–methane interaction.

If we are correct in suggesting that the Jensen and Jorgensen Li<sup>+</sup> parameters may have been compromised by the subsequent change in the experimentally accepted position of the Li<sup>+</sup>–water oxygen RDF, it highlights an unavoidable danger faced by all simulation practitioners involved in the parametrization of force fields: even the most carefully derived parameter sets can be

brought into question if the source experimental data are later revised. In passing, we note that for  $\text{Na}^+$  and  $\text{K}^+$  we observe no qualitative differences between the predictions of the Jensen and Jorgensen parameters and those of other tested parameter sets (data not shown).

Of course, an important caveat to the above discussion is that we still cannot state with any certainty that the thermodynamically favorable  $\text{Li}^+$ –methane interaction predicted in Figure 1a is correct; it is quite possible, for example, that despite the apparently incorrect hydration number obtained with the Jensen and Jorgensen parameters that its prediction of an unfavorable interaction might ultimately prove to be realistic. Given that the highly charge-dense nature of the  $\text{Li}^+$  ion is likely to induce some degree of electronic polarization in nearby water molecules, it may be that a resolution of this uncertainty might be forthcoming from the use of one or more of the polarizable force fields which are actively being developed in a number of laboratories;<sup>30,34</sup> it is also possible, however, that a quantum mechanical treatment might be required.<sup>31,32</sup>

## CONCLUSIONS

Despite the above caveat, we can state clearly that those parameter sets that currently appear to be more realistic—at least in terms of their structural description of  $\text{Li}^+$ 's interaction with water—predict a more thermodynamically favorable interaction between  $\text{Li}^+$  and methane. We can further state that an examination of the structure of the favorable  $\text{Li}^+$ –methane complex shows it to represent a fundamentally new mode of molecular interaction that appears halfway between a van der Waals contact and a solvent-separated interaction. We can also assert, from the results shown in Figure 1b and c, that similar kinds of favorable interaction are not obtained with either  $\text{Na}^+$  or  $\text{K}^+$  and, on the basis of additional simulations reported in the Supporting Information, that a favorable interaction is also not predicted for methane's interaction with the most charge-dense of the group VII anions,  $\text{F}^-$ , or with the  $\text{NH}_4^+$  ion (Figures S5 and S6, respectively, Supporting Information). Given that simulation results reported by others also show no evidence of a favorable interaction between methane and  $\text{Cl}^-$  or  $(\text{CH}_3)_4\text{N}^+$ ,<sup>4</sup> the predicted formation of a favorable short-range interaction between a monovalent ion and a hydrophobic molecule in aqueous solution appears to be unique to the  $\text{Li}^+$  ion.

In closing, we note that the unusual interaction observed here between  $\text{Li}^+$  and hydrophobic molecules provides an intriguing potential explanation for the finding that  $\text{Li}^+$  salts can act to denature a protein even when the corresponding  $\text{Na}^+$  and  $\text{K}^+$  salts serve as stabilizers.<sup>35</sup> In addition, the same interaction may well be an important factor in determining  $\text{Li}^+$ 's anomalously low salting-out ability.<sup>19b,36</sup> Finally, it provides yet another example of the subtle and sometimes highly surprising ways in which hydration-shell water molecules can mediate—both structurally and thermodynamically—the interactions of ions<sup>37</sup> or biomolecular solutes<sup>38</sup> in aqueous solution.

## ASSOCIATED CONTENT

**S** Supporting Information. Interaction free energies for  $\text{Li}^+$  with methane using altered van der Waals parameters, mixing rules, and box size dependence; energy decompositions of  $\text{Li}^+$ –methane simulation snapshots; water coordination numbers around methane; and interaction free energies for  $\text{F}^-$  with methane and for  $\text{NH}_4^+$  with methane. This information is available free of charge via the Internet at <http://pubs.acs.org>

## AUTHOR INFORMATION

### Corresponding Author

\*E-mail: [adrian-elcock@uiowa.edu](mailto:adrian-elcock@uiowa.edu).

## ACKNOWLEDGMENT

Supported by NSF CAREER award 0448029 (A.H.E.).

## REFERENCES

- (1) Marcus, Y. *Chem. Rev.* **2009**, *109*, 1346–1370.
- (2) Joung, I. J.; Cheatham, T. E. *J. Phys. Chem. B* **2008**, *112*, 9020–9041.
- (3) Hribar, B.; Southall, N. T.; Vlatchy, V.; Dill, K. A. *J. Am. Chem. Soc.* **2002**, *124*, 12302–12311.
- (4) Shinto, H.; Morisada, S.; Higashitani, K. *J. Chem. Eng. Jpn.* **2005**, *38*, 465–477.
- (5) Lund, M.; Vácha, R.; Jungwirth, P. *Langmuir* **2008**, *24*, 3387–3391.
- (6) Hess, B.; Kutzner, C.; van der Spoel, D.; Lindahl, E. *J. Chem. Theory Comput.* **2008**, *92*, 435–447.
- (7) Berendsen, H. J. C.; Grigera, J. R.; Straatsma, T. P. *J. Phys. Chem.* **1987**, *91*, 6269–6271.
- (8) Jorgensen, W. L.; Chandrasekhar, J.; Madura, J. D.; Impey, R. W.; Klein, M. L. *J. Chem. Phys.* **1983**, *79*, 926–935.
- (9) Horn, H. W.; Swope, W. C.; Pitera, J. W.; Madura, J. D.; Dick, T. J.; Hura, G. L.; Head-Gordon, T. *J. Chem. Phys.* **2004**, *120*, 9665–9678.
- (10) Åqvist, J. *J. Phys. Chem.* **1990**, *94*, 8021–8024.
- (11) Berendsen, H. J. C.; Postma, J. P. M.; van Gunsteren, W. F.; Hermans, J. In *Interaction Models for Water in Relation to Protein Hydration*; Pullman, B., Ed.; Reidel Publishing Company: Dordrecht, The Netherlands, 1981; p 311.
- (12) Jensen, K. P.; Jorgensen, W. L. *J. Chem. Theory Comput.* **2006**, *2*, 1499–1509.
- (13) Jorgensen, W. L.; Maxwell, D. S.; Tirado-Rives, J. *J. Am. Chem. Soc.* **1996**, *118*, 11225–11236.
- (14) Jorgensen, W. L.; Madura, J. D.; Swenson, C. J. *J. Am. Chem. Soc.* **1984**, *106*, 6638–6646.
- (15) Essmann, U.; Perera, L.; Berkowitz, M. L.; Darden, T.; Lee, H.; Pederson, L. G. *J. Chem. Phys.* **1995**, *103*, 8577–8593.
- (16) (a) Nosé, S. *J. Chem. Phys.* **1984**, *81*, 511–519. (b) Hoover, W. G. *Phys. Rev.* **1985**, *31*, 1695–1697.
- (17) Parrinello, M.; Rahman, A. *J. Appl. Phys.* **1981**, *52*, 7182–7190.
- (18) Hess, B.; Bekker, H.; Berendsen, H. J. C.; Fraaije, J. G. E. M. *J. Comput. Chem.* **1997**, *18*, 1463–1472.
- (19) (a) Thomas, A. S.; Elcock, A. H. *J. Am. Chem. Soc.* **2006**, *128*, 7796–7806. (b) Thomas, A. S.; Elcock, A. H. *J. Am. Chem. Soc.* **2007**, *129*, 14887–14898. (c) Zhu, S.; Elcock, A. H. *J. Chem. Theory Comput.* **2010**, *6*, 1293–1306. (d) Thomas, A. S.; Elcock, A. H. *J. Phys. Chem. Lett.* **2011**, *2*, 19–24.
- (20) (a) Wang, J.; Cieplak, P.; Kollman, P. A. *J. Comput. Chem.* **2000**, *21*, 1049–1074. (b) Sorin, E. J.; Pande, V. S. *Biophys. J.* **2005**, *88*, 2472–2493.
- (21) (a) Ghosh, T.; Kalra, A.; Garde, S. *J. Phys. Chem. B* **2005**, *109*, 642–651. (b) Trzesniak, D.; Kunz, A.-P. E.; van Gunsteren, W. F. *ChemPhysChem* **2007**, *8*, 162–169. (c) Sobolewski, E.; Makowski, M.; Czaplowski, C.; Liwo, A.; Oldziej, S.; Scheraga, H. A. *J. Phys. Chem. B* **2007**, *111*, 10765–10774.
- (22) Martínez, J. M.; Pappalardo, R. R.; Marcos, E. S. *J. Am. Chem. Soc.* **1999**, *121*, 3175–3184.
- (23) Gallicchio, E.; Kubo, M. M.; Levy, R. M. *J. Phys. Chem. B* **2000**, *104*, 6271–6285.
- (24) Paschek, D. *J. Chem. Phys.* **2004**, *120*, 6674–6690.
- (25) Marcus, Y. *Biophys. Chem.* **1994**, *51*, 111.

- (26) (a) Guillot, B.; Guissani, Y.; Bratos, S. *J. Chem. Phys.* **1991**, *95*, 3643–3648. (b) Guo, G.-J.; Zhang, Y.-G.; Li, M.; Wu, C.-H. *J. Chem. Phys.* **2008**, *128*, 194504.
- (27) Dec, S. F.; Bowler, K. E.; Stadterman, L. L.; Koh, C. A.; Sloan, E. D. *J. Am. Chem. Soc.* **2006**, *128*, 414–415.
- (28) (a) Obst, S.; Bradaczek, H. *J. Phys. Chem.* **1996**, *100*, 15677–15687. (b) Du, H.; Rasaiah, J. C.; Miller, J. D. *J. Phys. Chem. B* **2007**, *111*, 209–217.
- (29) Varma, S.; Rempe, S. B. *Biophys. Chem.* **2006**, *124*, 192–199 and references therein.
- (30) (a) San-Román, M. L.; Carrillo-Tripp, M.; Saint-Martin, H.; Hernández-Cobos, J.; Ortega-Blake, I. *Theor. Chem. Acc.* **2006**, *115*, 177–189. (b) Lamoureux, G.; Roux, B. *J. Phys. Chem. B* **2006**, *110*, 3308–3322. (c) Yu, H.; Whitfield, T. W.; Harder, E.; Lamoureux, G.; Vorobyov, I.; Anisimov, V. M.; Mackerell, A. D., Jr.; Roux, B. *J. Chem. Theory Comput.* **2010**, *6*, 774–786.
- (31) (a) Rempe, S. B.; Pratt, L. R.; Hummer, G.; Kress, J. D.; Martin, R. L.; Redondo, A. *J. Am. Chem. Soc.* **2000**, *122*, 966–967. (b) Lyubartsev, A. P.; Laasonen, K.; Laaksonen, A. *J. Chem. Phys.* **2001**, *114*, 3120–3126.
- (32) Loeffler, H. H.; Rode, B. M. *J. Chem. Phys.* **2002**, *117*, 110–117.
- (33) Marcus, Y. *Chem. Rev.* **1988**, *88*, 1475–1498.
- (34) (a) Ponder, J. W.; Wu, C.; Ren, P.; Pande, V. S.; Chodera, J. D.; Schneiders, M. J.; Haque, I.; Mobley, D. L.; Lambrecht, D. S.; DiStasio, R. A.; Head-Gordon, M.; Clark, G. N. I.; Johnson, M. E.; Head-Gordon, T. *J. Phys. Chem. B* **2010**, *114*, 2549–2564. (b) Lopes, P. E. M.; Roux, B.; Mackerell, A. D., Jr. *Theor. Chem. Acc.* **2009**, *124*, 11–28.
- (35) Sedláč, E.; Žoldák, G.; Antalík, M.; Sprinzl, M. *Biochim. Biophys. Acta* **2002**, *1597*, 22–27.
- (36) Weisenberger, S.; Schumpe, A. *AIChE J.* **1996**, *42*, 298–300.
- (37) Fennell, C. J.; Bizjak, A.; Vlachy, V.; Dill, K. A. *J. Phys. Chem. B* **2009**, *113*, 6782–6791.
- (38) Otwinowski, Z.; Schevitz, R. W.; Zhang, R.-G.; Lawson, C. L.; Joachimiak, A.; Marmorstein, R. Q.; Luisi, B. F.; Sigler, P. B. *Nature* **1988**, *335*, 321–329.